Time Mismatch Effect in Linearity of Hybrid Envelope Tracking Power Amplifier

Junhyung Jeong, *Student Member, IEEE*, Girdhari Chaudhary, *Member, IEEE*, and Yongchae Jeong, *Senior Member, IEEE*

***Abstract*—In this letter, a linearity degradation according to the time mismatching between RF and envelope paths in the hybrid envelope tracking (ET) power amplifier (PA) has been mathematically analyzed. From analysis, an asymmetric IM3 level of ET PA can be found due to the time mismatching between RF and envelope paths and AM-to-PM distortion of PA. For the experimental demonstration, the hybrid ET PA was designed for a wideband code division multiple access downlink band operating at a center frequency of 2.14 GHz. For the accurate time matching, the group delay time adjustor (GDTA) with 5 ns variation was employed in front of the RF PA. In the experiment, 4.78 dB improvement of ACPR for 4-FAs (frequency allocations) WCMDA signal of 20 MHz channel bandwidth was obtained by the optimum group delay tuning of the GDTA.**

***Index Terms*—Class-E PA, envelope elimination and restoration, envelope tracking, group delay time adjustor, linearity.**

I. Introduction

In the highly advanced modern wireless communication systems, high data transmission speed and capacity are required in the limited frequency spectrum. Therefore, spectrally efficient complex modulation schemes are used, which generates high peak to average power ratio (PAPR) and wide channel bandwidth signal. As a result, the backed-off region efficiency becomes important and many trials to improve the backed-off region efficiency have been studied such as Doherty amplifier, out-phasing technique, envelope tracking (ET), and envelope elimination restoration (EER) [1]–[3]. Among these techniques, the EER and ET techniques suggested by Kahn are used to supply the modulated drain bias instead of the constant drain bias [3].

Basically the architectures of EER and ET transmitters are similar to each other except the input signal of the power amplifier (PA). In case of the EER, the constant envelope signal containing the phase information only is applied to the switched mode PAs such as class-D/E/F. However, in the ET, the complex modulated envelope signal is applied to linear PAs such as class-A/AB. The EER has the best efficiency in a wide range of output power, but the linearity degradation is severely affected by the time mismatching between RF and envelope paths whereas the ET is relatively less sensitive to the time mismatching.

The hybrid ET is the combination of ET and EER techniques, which consists of switching mode PA, envelope detector, and envelope amplifier (or bias modulator). The hybrid ET can provide moderate efficiency and linearity with less sensitive time mismatching. However, the linearity degradation due to the time mismatching between two paths cannot be ignored, so linearity enhancement techniques were required such as analog or digital predistortion techniques [4], [5]. Moreover, although some work considered the time mismatching between two paths, but the AM-to-PM effect of the RF PA was ignored.

In this letter, the linearity degradation of the hybrid ET PA due to the time mismatching between RF and envelope paths is mathematically analyzed and experimentally verified. From the analysis, asymmetric third-order intermodulation (IM3) characteristic is observed as a result of the tiny time mismatching and AM-to-PM factor (φ) of the RF PA.

Manuscript received April 08, 2015; accepted April 30, 2015. Date of publication June 10, 2015; date of current version August 05, 2015.

The authors are with Division of Electronics and Information Engineering, IT Convergence Research Center, Chonbuk National University, Jeonju, Chollabuk-do, Republic of Korea (e-mail: ycjeong@jbnu.ac.kr).

Color versions of one or more of the figures in this letter are available online at http://ieeexplore.ieee.org.

Digital Object Identifier 10.1109/LMWC.2015.2440661

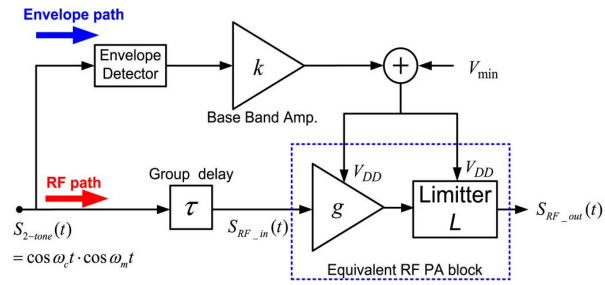

Fig. 1. Block diagram of the proposed hybrid envelop tracking architecture.

II. Mathematical Analysis

Fig. 1 shows the block diagram of the proposed hybrid ET system using Cann model [6], [7]. In this architecture, the time mismatching factor (τ) is included into the RF path in order to analyze the linearity degradation due to the time mismatching. From this model, the normalized two-tones modulated RF signal (S_{2_tone}), the drain bias voltage (V_{DD}), small signal gain (g), and saturated limiting level (L) of the RF PA are defined as

$$S_{2-\text{tone}}(t) = \cos\omega_c t \cdot \cos\omega_m t \quad (1)$$

$$V_{DD} = V_{\min} + k|\cos\omega_m t| \quad (2)$$

$$g = g_0 + g_1(V_{DD}) \quad (3)$$

$$L = L_0 + L_1(V_{DD}) \quad (4)$$

where ω_m, ω_c, and k are baseband modulation angular frequency, RF carrier angular frequency, and baseband amplifier voltage gain, respectively. As seen from (2), V_{DD} would be the amplified input envelope signal with the offset bias. Similarly, quantities of g and L are a function of V_{DD} and can be defined by I-V curve characteristics of the RF PA [7]. By using the Fourier expansion, (2) can be rewritten as (5), where only the second- and fourth-order terms are considered for simplicity.

$$V_{DD} = V_{\min} + k\left(a_0 + \sum_{n=2,4,6\cdots}^{\infty} a_n \cos n\omega_m t\right) \cong (V_{\min} + a_0 k) + a_2 k\cos 2\omega_m t + a_4 k\cos 4\omega_m t \quad (5)$$

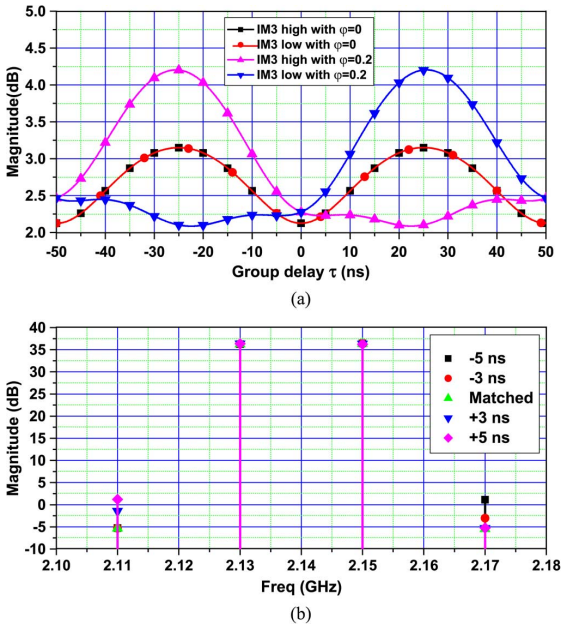

Fig. 2. (a) IM3 simulation results according to τ in condition of $\varphi = 0, 0.2$ and (b) measured IM3 variation according to ± 3 and ± 5 ns time mismatch.

TABLE I
SIMULATION PARAMETERS

Parameters	a_0	a_2	a_4	a_6	a_{10}
Values	2/π	4/3π	-4/15π	4/35π	15
Parameters	a_{11}	a_{30}	a_{31}	k	φ
Values	-1	-1.5	0.07	25	0.2

Finally, a nonlinear output signal of RF PA can be expressed as (6) by considering the nonlinear behavior and AM-to-PM factor φ of the RF PA from chapter 9.5 of [8]

$$S_{RF\_out}(t) = [\{a_{10}+a_{11}(V_{DD})\}\cos\{\omega_m(t-\tau)\} + \{a_{30}+a_{31}(V_{DD})\}\cos\{3\omega_m(t-\tau)\}] \cdot \cos\left[\omega_c(t-\tau) + \frac{\varphi}{2}(1+\cos\{2\omega_m(t-\tau)\})\right] \quad (6)$$

where a_{10}, a_{30} and a_{11}, a_{31} are fundamental, third-order output coefficients and correction coefficients according to V_{DD} variation, respectively

Furthermore, high and low third-order intermodulations ($IM3_{high}$ and $IM3_{low}$) with normalized input signal (1) can be expressed as (7) by using (6).

Fig. 2(a) shows the MATLAB simulation results of IM3s with τ using 7(a) and 7(b). In these calculations, f_m, f_c, and V_{min} are assumed as 10 MHz, 2.14 GHz, and 5 V, respectively. The used simulation parameters are given in Table I. When φ is assumed as zero, $IM3_{high}$ and $IM3_{low}$ have same magnitude at all τ ranges, which is similar to results presented in [1], [2]. But, asymmetric $IM3_{high}$ and $IM3_{low}$ outputs are occurred when φ is not zero and time mismatch. The $IM3_{high}$ and $IM3_{low}$ outputs according to the positive and negative τ are increased asymmetrically. The maximum $IM3_{high}$ and $IM3_{low}$ outputs are obtained at the quarter period of f_m (in this simulation, quarter periods of f_m are ± 25 ns), because the quarter period time mismatching means that the peak magnitude of the modulated RF signal is amplified with the minimum V_{DD} (or V_{min}) bias in the RF PA.

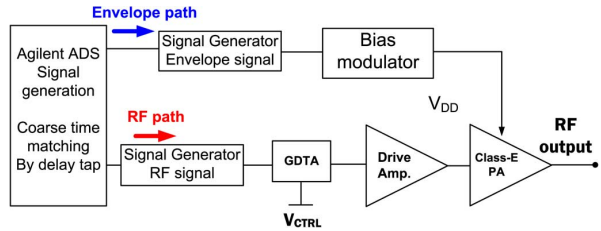

Fig. 3. Block diagram of experiment setup.

Fig. 2(b) shows the measured IM3s variation according to ± 3 and ± 5 ns time mismatches. The $IM3_{high}$ and $IM3_{low}$ are

$$IM3_{high} = \left[\frac{A}{2}\cos\left(\frac{\varphi}{2}-\omega_c\tau\right)+\frac{B}{2}\sin\left(\frac{\varphi}{2}-\omega_c\tau\right) + \frac{\varphi C}{8}\sin(\omega_c+2\omega_m)\tau\right]\cos(\omega_c+3\omega_m)t + \left[\frac{B}{2}\cos\left(\frac{\varphi}{2}-\omega_c\tau\right)-\frac{A}{2}\sin\left(\frac{\varphi}{2}-\omega_c\tau\right) - \frac{\varphi C}{8}\cos(\omega_c+2\omega_m)\tau\right]\sin(\omega_c+3\omega_m)t \quad (7a)$$

$$IM3_{low} = \left[\frac{A}{2}\cos\left(\frac{\varphi}{2}-\omega_c\tau\right)-\frac{B}{2}\sin\left(\frac{\varphi}{2}-\omega_c\tau\right) + \frac{\varphi C}{8}\sin(\omega_c-2\omega_m)\tau\right]\cos(\omega_c-3\omega_m)t - \left[\frac{B}{2}\cos\left(\frac{\varphi}{2}-\omega_c\tau\right)+\frac{A}{2}\sin\left(\frac{\varphi}{2}-\omega_c\tau\right) + \frac{\varphi C}{8}\cos(\omega_c-2\omega_m)\tau\right]\sin(\omega_c-3\omega_m)t \quad (7b)$$

where

$$A = \frac{ka_{11}a_2}{2}\cos\omega_m\tau + \frac{ka_{11}a_4}{2}\cos\omega_m\tau + (a_{30}+a_{31}V_{\min}+a_0a_{31}k)\cos 3\omega_m\tau + \frac{ka_{31}a_6}{2}\cos 3\omega_m\tau \quad (8a)$$

$$B = \frac{ka_{11}a_2}{2}\sin\omega_m\tau + \frac{ka_{11}a_4}{2}\sin\omega_m\tau + (a_{30}+a_{31}V_{\min}+a_0a_{31}k)\sin 3\omega_m\tau + \frac{ka_{31}a_6}{2}\sin 3\omega_m\tau \quad (8b)$$

$$C = a_{10} + a_{11}V_{\min} + a_0a_{11}k \quad (8c)$$

varying $-5.28 \sim 1.22$ dB and $-5.24 \sim 1.13$ dB with time mismatches. These IM3 variation ranges are larger than simulation results. Because in the theory, the limiter operation is ignored for a tiny time mismatch. But the actual output signal of PA is limited by an improper bias voltage signal with the time mismatch, so that it generates additional distortions. IM3 deviation ranges in measurement results are larger than simulation results.

III. EXPERIMENTAL RESULTS

To validate the mathematical analysis of the IM3 degradation due to τ, the nonlinear hybrid ET PA was designed for a wideband code division multiple access (WCDMA) downlink band operating at 2.14 GHz. Fig. 3 shows the block diagram of the experimental setup. Two signal generators were used for RF and envelope signals generation. For the experiment, the class-E PA was designed with a defect ground structure (DGS) on the output matching network [9]. The 2nd to 5th harmonics are relatively open to the fundamental load impedance by DGS. The PA was designed with a gallium nitride high electron mobility transistor NPTB00025 of Nitronex, which had a peak output power of 25 W. The measured maximum output power, gain,

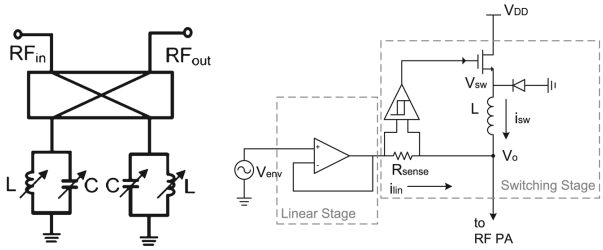

(a) (b)

Fig. 4. Block diagram of (a) single stage reflective type group delay time adjustor and (b) bias modulator.

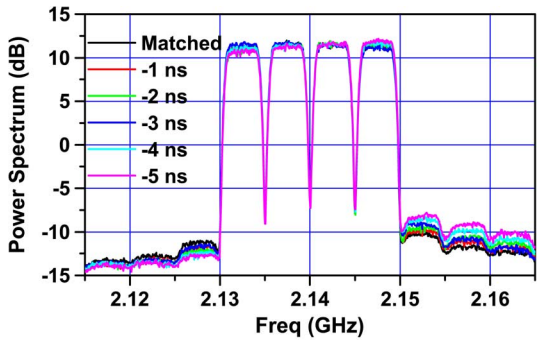

(a)

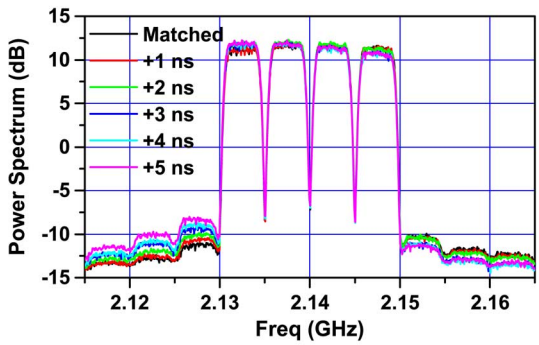

(b)

Fig. 5. The measured output spectrums for WCDMA 4-FAs signals with group delay variations of (a) $0 \sim -5$ ns and (b) $0 \sim +5$ ns.

drain efficiency, and power added efficiency of the RF PA were 43.1 dBm, 11.41 dB, 74.36%, and 69.11%, respectively.

Although a coarse time matching can be achieved by ADS delay tap, cable, and signal generators before connecting to the bias modulator and RF PA, a precise time matching is required to optimize the ET system performance. For obtaining the precise time matching between two paths, 2-stage group delay time adjustor (GDTA) that can control a group delay time continuously was inserted in front of the RF PA [10]. Block diagram of single stage GDTA is show in Fig. 4(a). The fabricated GDTA provides a group delay of 3.7–8.7 ns with an insertion loss lower than 0.5 dB over a bandwidth of 60 MHz.

Fig. 4(b) represents a block diagram of bias modulator [11]. The current to the RF PA is determined by the combination of switching stage current (i_{sw}) and linear stage current (i_{lin}), but most of DC current is provided from the switching stage by the buck converter operation and the linear stage is operated by the op-amp as a voltage source. By detecting the current direction on a hysteresis operation, i_{sw} can be determined. Measured 3 dB small signal bandwidth of bias modulator is 178 MHz.

Fig. 5 shows the measured output spectrums of the fabricated hybrid ET PA for the WCDMA 4-FAs signal (total signal bandwidth: 20 MHz, PAPR: 9.6 dB) with τ of ± 5 ns, where τ of 0 ns is the time matching condition (balanced pass band spectrum with optimized ACPR). As τ is deviated from the time matching condition, asymmetrical output spectrum characteristic is distinct. From measurements, 4.48 dB and 4.78 dB of ± 5 MHz ACPR degradation are observed at the back-offed average output power of 33.5 dBm, drain efficiencies of $41.2 \sim 40.3\%$ with τ of $\pm$ 5 ns variations. Detail measurement data are shown in Table II.

TABLE II
ACPR PERFORMANCES ACCORDING TO MISMATCHING TIMES FOR WCDMA 4-FAS

Mismatching time[ns]	- 5MHz ACPR [dBc]	+ 5MHz ACPR [dBc]
+5	20.2	24.78
+4	20.45	24.28
+3	21.19	23.89
+2	21.68	23.4
+1	21.91	22.92
0(matched)	22.29	22.45
-1	22.96	21.92
-2	23.63	21.52
-3	24.19	21.19
-4	24.56	20.62
-5	24.98	20.3

IV. CONCLUSION

In this letter, the linearity degradation for the hybrid envelope tracking PA due to the time mismatching between RF and envelope paths is analyzed mathematically and verified experimentally. From the analysis, asymmetrical output spectrum is evident due to the time mismatching between two paths and AM-to-PM factor of the RF PA. To obtain the time matching, 2-stage group delay time adjustor is used in the RF path. The linearity of the hybrid envelope tracking system can be improved by the time match between two paths and it can reduce the memory effect(asymmetrical IM3) of the nonlinear RF PA. Moreover, asymmetrical IM3s or ACPR characteristics can be compensated by intended time mismatch

REFERENCES

[1] F. H. Raab, "Efficiency of outphasing RF power-amplifier systems," *IEEE Trans. Comm.*, vol. com-33, no. 10, pp. 1094–1099, Oct. 1985.
[2] F. H. Raab, P. Asbeck, S. Cripps, P. B. Kenington, Z. Popovic, N. Pothecary, J. F. Sevic, and N. O. Sokal, "Power amplifiers and transmitters for RF and microwave," *IEEE Trans. Microw. Theory Tech.*, vol. 50, no. 3, pp. 814–826, Mar. 2002.
[3] F. H. Raab, "Intermodulation distortion in Kahn-technique transmitters," *IEEE Trans. Microw. Theory Tech.*, vol. 44, no. 12, pp. 2273–2278, Dec. 1996.
[4] K. Chen, K. A. Morris, and M. A. beach, "Combining envelope elimination and restoration and predistortion techniques for use in IEEE 802.11g systems," *IET Microw. Antennas Propag.*, vol. 1, no. 4, pp. 832–838, Aug. 2007.
[5] A. Zhu, P. J. Draxler, C. Hsia, T. J. Brazil, D. F. Kimball, and P. Asbeck, "Digital predistortion for envelope-tracking power amplifiers using decomposed piecewise Volterra series," *IEEE Trans. Microw. Theory Tech.*, vol. 56, no. 10, pp. 2237–2247, Oct. 2008.
[6] A. J. Cann, "Improved nonlinearity model with variable knee sharpness," *IEEE Trans. Aerosp. Electron. Syst.*, vol. 48, no. 4, pp. 3637–3646, Oct. 2012.
[7] F. Wang, A. H. Yang, D. F. Kimball, L. E. Larson, and P. Asbeck, "Design of wide-bandwidth envelope-tracking power amplifier for OFDM applications," *IEEE Trans. Microw. Theory Tech.*, vol. 53, no. 4, pp. 1244–1255, Apr. 2005.
[8] S. C. Cripps, *RF Power Amplifiers for Wireless Communications*, 2nd ed. Norwood, MA: Artech House, 2007.
[9] H. Choi, S. Shim, Y. Jeong, J. Lim, and C. D. Kim, "A compact DGS load-network for highly efficient class-E power amplifier," in *Proc. of European Microwave Conference*, Sep. 2009, pp. 492–495.
[10] G. Chaudhary, H. Choi, Y. Jeong, J. Lim, and C. D. Kim, "Design of group delay time controller based on reflective parallel resonator," *ETRI Journal*, vol. 34, no. 2, pp. 210–215, Apr. 2012.
[11] Y. Li and D. Maksimovic, "High efficiency wide bandwidth power supplies for GSM and EDGE RF power amplifier," in *IEEE International Symposium on Circuits and Systems*, May 2005, vol. 2, pp. 1314–1317.